Ollscoil na Gaillimhe
University of Galway

Provided by the author(s) and University of Galway in accordance with publisher policies. Please cite the published version when available.

Title	Proactive esophageal cooling during laser cardiac ablation: A computer modeling study
Author(s)	Gomez Bustamante, Tatiana; Mercado Montoya, Marcela; Berjano, Enrique; González Suárez, Ana; Kulstad, Erik
Publication Date	2024-03-04
Publication Information	Gomez Bustamante, Tatiana, Mercado Montoya, Marcela, Berjano, Enrique, González-Suárez, Ana, & Kulstad, Erik. Proactive esophageal cooling during laser cardiac ablation: A computer modeling study. Lasers in Surgery and Medicine, n/a(n/a). doi: https://doi.org/10.1002/lsm.23774
Publisher	Wiley
Link to publisher's version	https://doi.org/10.1002/lsm.23774
Item record	http://hdl.handle.net/10379/18088
DOI	http://dx.doi.org/10.1002/lsm.23774

Downloaded 2024-05-20T15:08:31Z

Some rights reserved. For more information, please see the item record link above.

Proactive esophageal cooling during laser cardiac ablation:

A computer modeling study

Tatiana Gomez Bustamante[1], Marcela Mercado Montoya[1], Enrique Berjano[2],

Ana González-Suárez[3,4], Erik Kulstad[5]

[1] *In Silico Science & Engineering S.A.S., Medellin, Colombia*
[2] *BioMIT, Department of Electronic Engineering, Universitat Politècnica de València, Spain*
[3] *Translational Medical Device Lab, Lambe Institute for Translational Research, School of Medicine, University of Galway, Ireland*
[4] *Valencian International University, Valencia, Spain*
[5] *University of Texas Southwestern Medical Center, Dallas, TX, USA*

ORCID numbers:
Tatiana Gomez Bustamante: 0000-0002-3947-1390
Marcela Mercado Montoya: 0000-0002-1453-4690
Enrique Berjano: 0000-0002-3247-2665
Ana González-Suárez: 0000-0002-1813-4176
Erik Kulstad: 0000-0002-9331-8266

Corresponding author: Tatiana Gómez Bustamante. In Silico Science & Engineering S.A.S., CL 52 81 48, Medellín, Colombia, 050035.

Funding details: Research reported in this publication was supported by the National Heart, Lung and Blood Institute of the National Institutes of Health under Award Number R44HL158375 (the content is solely the responsibility of the authors and does not necessarily represent the official views of the National Institutes of Health) and the Spanish Ministerio de Ciencia e Innovación, Agencia Estatal de Investigación, Fondo Europeo de Desarrollo Regional (Grants PID2022-136273OB-C31 and PID2022-136273OA-C33 funded by MCIN / AEI/ 10.13039/501100011033 / FEDER, UE).
Conflicts of interest: MMM and TGB: employment with In Silico SE, consulting for Attune Medical; EK: equity and employment in Attune Medical. The rest of the authors declare no conflict of interest.
Running title: Esophagus damage provoked by laser cardiac ablation.
Data availability: Supplementary material (Excel file) includes the raw data of the simulation and verification of the model, along with video files showing the progresses of the variables during the transient simulation.

ABSTRACT

Background and objectives: Laser ablation is increasingly used to treat atrial fibrillation (AF). However, atrioesophageal injury remains a potentially serious complication. While proactive esophageal cooling (PEC) reduces esophageal injury during radiofrequency ablation, the effects of PEC during laser ablation have not previously been determined. We aimed to evaluate the protective effects of PEC during laser ablation of AF by means of a theoretical study based on computer modeling.

Methods: Three-dimensional mathematical models were built for 20 different cases including a fragment of atrial wall (myocardium), epicardial fat (adipose tissue), connective tissue and esophageal wall. The esophagus was considered with and without PEC. Laser-tissue interaction was modeled using Beer-Lambert's law, Pennes' Bioheat equation was used to compute the resultant heating, and the Arrhenius equation was used to estimate the fraction of tissue damage (FOD), assuming a threshold of 63% to assess induced necrosis. We modeled laser irradiation power of 8.5 W over 20 s. Thermal simulations extended up to 250 s to account for thermal latency.

Results: PEC significantly altered the temperature distribution around the cooling device, resulting in lower temperatures (around 22 ºC less in the esophagus and 9 °C in the atrial wall) compared to the case without PEC. This thermal reduction translated into the absence of transmural lesions in the esophagus. The esophagus was thermally damaged only in the cases without PEC and with a distance equal to or shorter than 3.5 mm between the esophagus and endocardium (inner boundary of the atrial wall). Furthermore, PEC demonstrated minimal impact on the lesion created across the atrial wall, either in terms of maximum temperature or FOD.

Conclusions: PEC reduces the potential for esophageal injury without degrading the intended cardiac lesions for a variety of different tissue thicknesses. Thermal latency may influence lesion formation during laser ablation and may play a part in any collateral damage.

Key words: Atrial fibrillation; atrioesophageal fistula; esophageal cooling; laser balloon; laser ablation; mathematical modeling.

ABBREVIATIONS

AF : Atrial fibrillation

AEF : Atrioesophageal fistula

FEM : Finite element method

RF : Radiofrequency

Nd :YAG: Neodymium-doped yttrium aluminum garnet

T : Temperature

ρ : Density

C_{eff} : Effective specific heat capacity

ρ_{ref} : Density for each tissue

C_{ref} : Specific heat capacity for each tissue

k : Thermal conductivity

Q_P : Blood perfusion

Q_L : Laser-induced heat source

Q_M : Metabolic heat

$\boldsymbol{u}$: Velocity vector

ρ_{bl} : Blood density

$C_{p,bl}$: Blood heat capacity

ω_{bl} : Perfusion rate

T_{bl} : Blood temperature

β : Non-dimensional parameter to simulate that blood perfusion cessation

T_b : Body temperature

ε : Surface emissivity

σ : Stefan–Boltzmann constant

z : Depth into the tissue

I_Z : Laser irradiance

μ_{eff} : Effective attenuation coefficient

μ_a : Coefficient of absorption

μ_{rs} : Reduced scattering coefficient

μ_s : Scattering coefficient

g : Anisotropy coefficient

r_i : Radius of the laser applicator

I_0 : Irradiation intensity in the surface

P : Applied laser power

α : Degree of thermal damage

A : Frequency factor

E_a : Activation energy

n : Reaction order

R : Gas constant

FOD, θ_d : Fraction of damage

L_w : Water latent heat

W : Water content

INTRODUCTION

Atrial fibrillation (AF) is one of the most common arrhythmias. One of the treatment options is catheter ablation, which is clinically conducted by delivering energy (radiofrequency, microwave, laser, or high-intensity voltage pulses) in a minimally invasive way. Note that unlike other ablative energies such as radiofrequency or microwave, lasers are often used to eliminate tissue (excision by volatilization). This is not the case in cardiac ablation, in which the term ablation does not imply "removal". Instead, it is a tissue damage that results in loss of electrical activity, but the tissue remains, subsequently undergoing fibrosis or scar formation. During AF ablation, energy is applied near the posterior wall of the left atrium, which is anatomically very close to the esophagus (see Fig. 1). In fact, atrioesophageal fistula (AEF) remains a potentially serious complication from atrial fibrillation (AF) ablation. AF ablation balloon-based laser is a relatively new technology compared to radiofrequency (RF) or cryotherapy [1], with less clinical experience on safety and efficacy [2]. Since AEF is suspected to be mainly provoked by heat, it is reasonable to assume that the energy of the laser beam might cause thermal damage to the esophagus in cases where the esophagus is very close to the atrial wall [3]. The potential damage to the esophagus during laser ablation has been less well studied. To the best of our knowledge, only the study by Weber *et al* [4] addressed this issue using preclinical experimental models (*ex vivo* and *in vivo*), concluding that potentially dangerous temperatures can be reached in the esophagus, and that damage can be minimized using extremely low power levels (150 μW), which are lower than those usually used in the clinic, e.g.

using the Nd:YAG laser balloon catheter model HeartLight X3 (CardioFocus, Marlborough, MA, USA) [5].

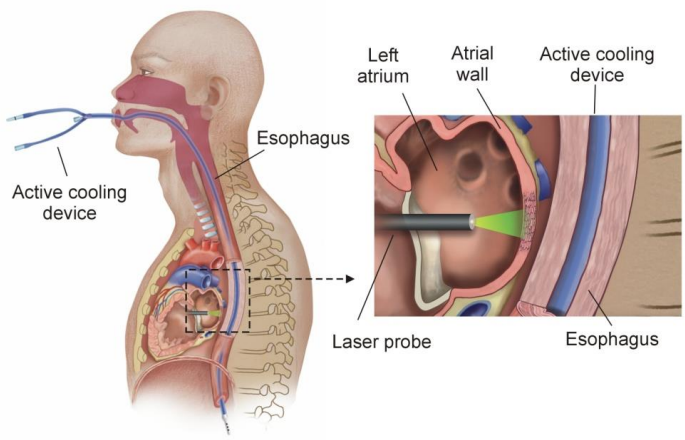

Figure 1. Physical situation during laser ablation to treat atrial fibrillation with an active cooling device located in the esophageal lumen to prevent thermal damage.

Computer modeling has been previously used to assess the thermal insult of RF on the esophagus during AF ablation [6], along with the positive impact of using esophageal cooling devices [7–9]. Since laser energy interacts with biological tissues in a different way than RF energy, it is crucial to assess the potential damage of laser ablation on the esophagus as well as the potential benefit of using esophageal cooling. In contrast to the method of instilling cold water into the esophagus in response to temperature elevations measured with a thermometer (reactive cooling), proactive esophageal cooling (PEC) employs a dedicated cooling device that continuously cools the esophageal mucosa prior to initiating thermal ablation in the heart (see Fig. 1). The cooling device circulates chilled water in a multi-lumen closed-loop system. Water flow at a rate of greater than 60 liters per hour passes through the device at a setpoint temperature of 4

ºC. The chilled water is supplied by an external heat exchanger through connection tubing, and the entirety of the length of the cooling device (which is in contact with the esophageal mucosa) is cooled to the temperature of the water. As such, the entire esophagus is cooled continuously to 4 ºC, providing a continuous conductive cooling of the esophagus. Cooling is typically initiated 3–5 minutes prior to the start of ablation, allowing equilibration of temperature between device and esophageal mucosa to occur, and cooling continues until after the ablation has been completed. There are no previous computer modeling studies aimed at assessing the thermal damage to the esophagus during laser ablation of AF. Our goal was hence to evaluate using computer modeling the effects of PEC on thermal damage in the esophagus during ablation with a laser balloon, testing different tissue thicknesses which represent the anatomical variability present in the clinical setting.

METHODS

We used mathematical modeling to study the physical phenomena involved during laser balloon ablation of the left atrium with and without PEC for 20 different sets of tissue thicknesses while considering thermal latency (lesion growth occurring after power ceases). 3D models were built and solved using the Finite Element Method (FEM) with the software COMSOL Multiphysics (COMSOL, Burlington, MA, USA). The model uses Pennes' Bioheat equation and includes accommodations for the phase change of tissues during thermal ablation. Laser-tissue interaction was computed using Beer Lambert's Law, and tissue damage was calculated with the Arrhenius formula (see details below).

Model geometry

Figure 2 shows the model domains, including all the relevant tissues and their proximity to the ablation target: atrial wall, epicardial fat, connective tissue and esophagus. No blood was included since in the real clinical scenario the inflated balloon displaces blood, simply leaving its outer plastic surface resting on the endocardium. A cylindrical structure was assumed to be embedded into the connective tissue in order to model the esophageal lumen occupied by an active cooling device (ensoETM, Attune Medical, Chicago, IL, USA). This device was modeled as a hollow silicone tube (1.2 cm diameter, 0.65 mm wall thickness) full of cold water, which is circulated by a pump. Control conditions, in which no PEC was present, were modeled by a collapsed esophagus. In this case, the subdomain corresponding to the cooling device was replaced with the properties of "esophagus and other tissues".

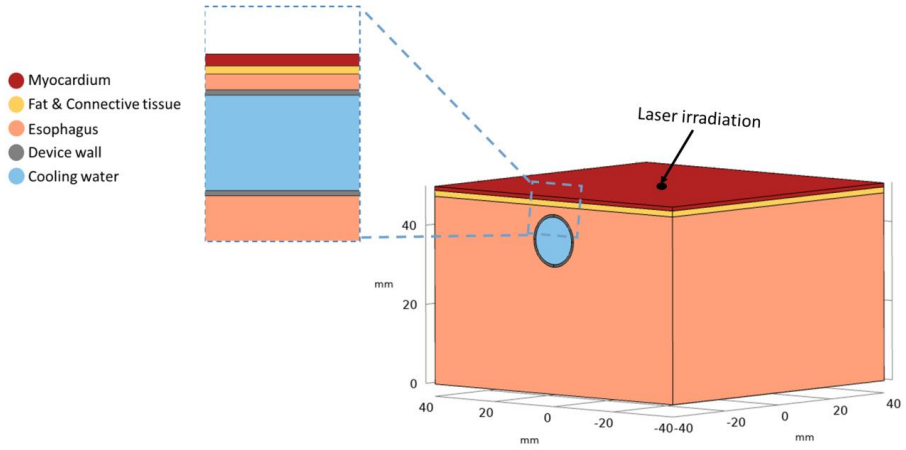

Figure 2. Model geometry showing the subdomains (which are made up of different materials) near the ablation site and the active cooling device located in the esophageal lumen.

The model considered that the atrial wall surface is irradiated with an Nd:YAG laser balloon catheter such as HeartLight X3 (CardioFocus, Marlborough, MA, USA) in manual mode, i.e. delivering a fixed dose (power) for a fixed amount of time (seconds). Specifically, we considered 8.5 W for 20 s that in Manual mode should be used as a starting dose in most ablation procedures [5]. These values are exactly those used by Nagase *et al* [10] in a laser balloon ablation in vitro experiment to evaluate lesion size comparing different energy settings. We considered a point application, i.e. without dragging and without overlapping since only a single application was considered. The tissue was assumed to be heterogeneous, constituted by layers of different thicknesses according to anatomical data. Specifically, from the endocardium inward: 1) with thicknesses of 1.0, 1.5 and 2.0 mm [11], and 2) fat and connective tissue, modeled under the same properties, from 1.5 to 5 mm [11], to set distances between endocardium and the outer esophageal surface ranging from 2.5 to 7 mm [11,12]. Table 1 shows the anatomical details of the 20 cases considered, i.e. thicknesses of the atrial wall, epicardial fat and connective tissue between fat and esophagus.

Table 1. Lesion depth (mm) and percentage of damaged esophageal wall for the 20 cases under consideration, testing different thicknesses of the atrial wall, epicardial fat and connective tissue (in bold those cases in which esophageal damage occurred, as measured by the percentage of tissue for which the FOD is greater than or equal to 63%) for both control and protection conditions (without and with PEC, respectively).

Cases	Tissues layers (Dimensions in mm)		Lesion depth (mm)				% Damaged esophagus	
			Control		Protection			
	Atrial wall	Fat + Connective tissue	20 s	250 s	20 s	250 s	Control	Protection
1	1.0	1.5	3.46	3.70	1.00	1.00	**60%**	0%
2	1.0	2.5	1.00	3.63	1.00	1.00	**6%**	0%
3	1.0	3.5	1.00	1.00	1.00	1.00	0%	0%
4	1.0	4.5	1.00	1.00	1.00	1.00	0%	0%
5	1.0	5.5	1.00	1.00	1.00	1.00	0%	0%
6	1.5	1.0	3.42	3.66	1.50	1.50	**58%**	0%
7	1.5	2.0	1.50	3.57	1.50	1.50	**3%**	0%
8	1.5	3.0	1.50	1.50	1.50	1.50	0%	0%
9	1.5	4.0	1.50	1.50	1.50	1.50	0%	0%
10	1.5	5.0	1.50	1.50	1.50	1.50	0%	0%
11	2.0	0.5	3.37	3.60	1.66	1.81	**55%**	0%
12	2.0	1.0	3.26	3.51	2.00	2.00	**26%**	0%
13	2.0	1.5	2.00	3.500	2.00	2.00	0%	0%
14	2.0	2.0	2.00	2.00	2.00	2.00	0%	0%
15	2.0	2.5	2.00	2.00	2.00	2.00	0%	0%
16	2.0	3.0	2.00	2.00	2.00	2.00	0%	0%
17	2.0	3.5	2.00	2.00	2.00	2.00	0%	0%
18	2.0	4.0	2.00	2.00	2.00	2.00	0%	0%
19	2.0	4.5	2.00	2.00	2.00	2.00	0%	0%
20	2.0	5.0	2.00	2.00	2.00	2.00	0%	0%

Physical phenomena and governing equations

The Bioheat equation and Beer-Lambert's Law were used to solve thermal and optical phenomena involved during laser ablation, respectively. The degree of thermal damage was calculated using the Arrhenius model [9].

Bioheat phenomena

The thermal problem was computed in all the subdomains (see Figure 2) using the Pennes' Bioheat equation [13]:

$$\rho C_{eff}\frac{\partial T}{\partial t} + \nabla \cdot (-k\nabla T) = Q_P + Q_L + Q_M \quad (1)$$

where T is the temperature (ºC), ρ is the density (kg·m^{-3}), C_{eff} is the effective specific heat capacity at constant pressure (J·kg^{-1}·K^{-1}), k is the thermal conductivity (W·m^{-2}·K^{-1}), Q_P is the blood perfusion term (W·m^{-3}) and Q_L the laser-induced heat source (W·m^{-3}), which is only active during the laser pulse duration. The metabolic heat Q_M (W·m^{-3}) is negligible compared to the energy dissipation and was hence ignored [14].

A term corresponding to thermal advection was considered specifically for the subdomain corresponding to the cold circulating water, at 4 ºC (i.e. inside the silicone tube), leaving the Eq. (1) as follows:

$$\rho C_{eff}\frac{\partial T}{\partial t} + \nabla \cdot (-k\nabla T) + \rho C_p \boldsymbol{u} \cdot \nabla T = Q_P + Q_L \quad (2)$$

where $\boldsymbol{u}$ is the velocity field for this subdomain (m·s^{-1}), which is obtained from the inner area of the tube and the rate used in clinics (60 L/h).

The source term for perfusion in Eq. (2) Q_P was computed as follows:

$$Q_p = \beta \rho_{bl} C_{p,bl} \omega_{bl} (T_{bl} - T) \quad (3)$$

where ρ_{bl} is blood density, $C_{p,bl}$ is blood heat capacity, ω_{bl} is the perfusion rate, taken from the IT'IS database for each tissue [15], T_{bl} is blood temperature (37 ºC) and β is a non-dimensional parameter to simulate that blood perfusion ceases once tissue is completely destroyed by thermal necrosis (β = 1 while fraction of thermal damage remains less than 99% and β = 0 for 100% damage) [9].

A radiation boundary condition was considered on the atrial wall exterior surface, to account for the heat dissipation from the tissue, as follows:

$$-n \cdot (-k\nabla T) = \varepsilon\sigma(T_b^4 - T^4) \quad (4)$$

where T_b is body temperature (37 ºC), ε is surface emissivity (0.8) [16] and σ is the Stefan–Boltzmann constant (5.6703×10^{-8} W·m^{-2}·K^{-4}). Outer boundaries were set to T_b = 37 ºC. A 37 °C boundary condition was set in the outer walls of the model, to guarantee body temperature at the far away boundaries. To account for the cooling water flow, without considering Navier Stokes equation, a simplification was made setting an inflow boundary condition at 4 °C (device cooling temperature) at the device inlet boundary, and an outflow at the device outlet boundary.

Optical phenomena

Beer-Lambert's Law was used to model the absorption of energy in the tissue. To do that, a heat source Q_L was considered in Eq. (2), which includes the coefficient of absorption (μ_a m^{-1}), laser irradiance I_z (power received by the tissue surface per unit area) and the effective attenuation coefficient μ_{eff}, since the biological tissues are not only absorptive, but also exhibit significant scattering behavior particularly in regions of high tissue density or complex microstructures [17,18].

$$Q_L = \mu_a I_z e^{-\mu_{eff} z} \quad (5)$$

where z is the depth into the tissue (m), I_Z is the laser irradiance (W·m^{-2}), and μ_{eff} is the effective attenuation coefficient (m^{-1}), which includes the coefficients of absorption (μ_a m^{-1}), related to the energy absorbed by chromophores, such as hemoglobin or melanin, and reduced scattering coefficient μ_{rs}, that can be expressed in terms of scattering (μ_s) and anisotropy coefficients (g); the former determines how light scatters within the tissue, affecting the distribution and depth of laser energy, and the latter indicates the directionality of scattering. Tissue optical properties were considered for an Nd:YAG wavelength of 1064 nm [18,19]

$$\mu_{eff} = \sqrt{3\mu_a(\mu_a + \mu_{rs})} \quad (6)$$

$$\mu_{rs} = \mu_s(1 - g) \quad (7)$$

The laser irradiance I_Z (W·m^{-2}) represented as a 2D Gaussian distribution, was applied as a boundary condition on the atrial wall exterior surface, representing the power per unit area of the incident laser light, determining the rate at which laser energy is delivered to tissues [20]:

$$I_z = I_0 e^{-\frac{2(x^2+y^2)}{(\frac{r_i}{3})^2}} \quad (8)$$

where r_i is the radius of the laser applicator, divided by three, to obtain the 99% of the output laser power [18], and I_0 (W·m^{-2}) is the irradiation intensity in the surface defined as:

$$I_0 = \frac{2P}{\pi(\frac{r_i}{3})^2} \quad (9)$$

where P is the laser power (W).

Tissue damage

The degree of thermal damage α was described according to the Arrhenius formulation shown in Eq. (10), considering two different sets of parameters, one for the fat and connective tissue, and the other for myocardium (atrial wall) and esophagus [9].

$$\frac{\partial \alpha}{\partial t} = Ae^{-\frac{E_a}{RT}}(1-\alpha)^n \quad (10)$$

where A is frequency factor (s^{-1}), E_a is activation energy ($J \cdot mol^{-1}$), n is the reaction order ($n = 1$) and R is the gas constant (8.3145 $J \cdot mol^{-1} \cdot K^{-1}$). Values of 0.63 (63%) and 0.99 (99%) are commonly used to represent permanent tissue damage. Lesion sizes were estimated at 250 s after laser irradiation to account for additional lesion growth due to thermal latency. The fraction of damage (FOD) θ_d, ranging from 0 and 1, was calculated as the maximum value between zero and the maximum between α and 1, as follows:

$$\theta_d = max\{0, (\alpha, 1)\} \quad (11)$$

Tissue damage was considered for FOD greater than or equal to 0.63 (or 63%).

Material properties

The variation with temperature of the density and thermal conductivity were considered for all the tissues. These variations were represented using the following equations with the temperature T (in ºC):

$$k = k_{ref} \cdot [1.0 + 1.20 \times 10^{-3} \cdot (T - 37.0)] \quad (12)$$

$$\rho = \frac{k}{C_{ref} \cdot 1.474\times10^{-7} \cdot [1.0+3.39\times10^{-3} \cdot (T-37.0)]} \quad (13)$$

At high temperature regions, less energy is absorbed due to loss of tissue water [21]. To account for evaporation attributed to the change in water content due to increased temperature, an effective specific heat capacity C_{eff} is considered as shown in Eq. (3) [22].

$$C_{eff} = C_{ref} - \frac{L_w}{\rho_{ref}} \frac{\partial W}{\partial T} \quad (14)$$

where C_{ref} and ρ_{ref} are the heat capacity and density for each tissue respectively, L_w is the water latent heat (2260 kJ·kg^{-1}), and $\frac{\partial W}{\partial T}$ is the change in water content due to temperature, as shown in Figure 3 [23].

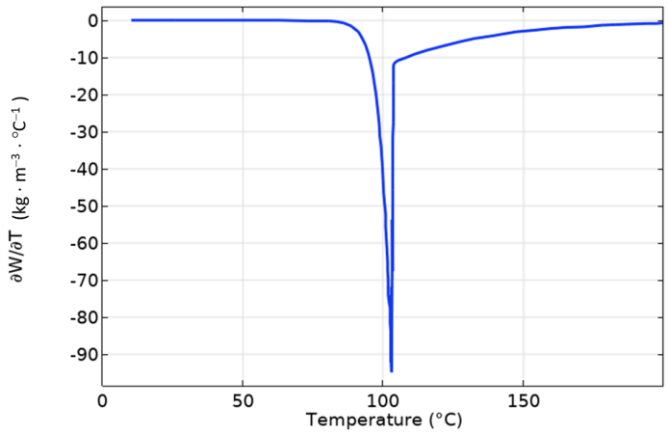

Figure 3. Change of water content ($\frac{\partial W}{\partial T}$) due to temperature, according to [23].

The reference values for the thermal conductivity (k_{ref}) and the heat capacity C_{ref}, as well as the optical properties (at 1064 nm), and Arrhenius parameters for each tissue, are shown in Table 2 [9,15,19,24].

Table 2. Thermal, optical, and Arrhenius properties for each tissue [9,15,19,24].

Tissue	**Thermal** [15]		**Optical** * [19,24]				**Arrhenius** [9]	
	k_{ref} (W·m^{-1}·K^{-1})	$C_{p,ref}$ (J·kg^{-1}·K^{-1})	μ_a (m^{-1})	μ_s (m^{-1})	g	μ_{rs} (m^{-1})	A (s^{-1})	E_a (J·mol^{-1})
Myocardium (atrial wall)	0.56	3686	30	17750	0.964	639	7.39×10^{39}	2.59×10^{5}
Fat + Connective tissue	0.21	2348	21	12710	0.933	851.57	4.43×10^{16}	1.30×10^{5}
Esophagus + Other tissues	0.53	3500	110	-	-	1162	7.39×10^{39}	2.59×10^{5}

* Tissue optical properties were considered for an Nd:YAG wavelength of 1064 nm.

Comentado [TG1]: Please change this reference for Sweer, J. A., Chen, M. T., Salimian, K. J., Battafarano, R. J., & Durr, N. J. (2019). Wide-field optical property mapping and structured light imaging of the esophagus with spatial frequency domain imaging. *Journal of biophotonics*, *12*(9), e201900005. https://doi.org/10.1002/jbio.201900005

The cooling device walls were considered as made of silicone, with predefined constant material properties of COMSOL ($\rho = 1240$ kg·m^{-3}, $k = 0.4$ W·m^{-1}·K^{-1}, $C_p = 1200$ J·kg^{-1}·K^{-1}), and the cooling water of the device was considered as temperature dependent, also according to the COMSOL material library, shown in Figure 4.

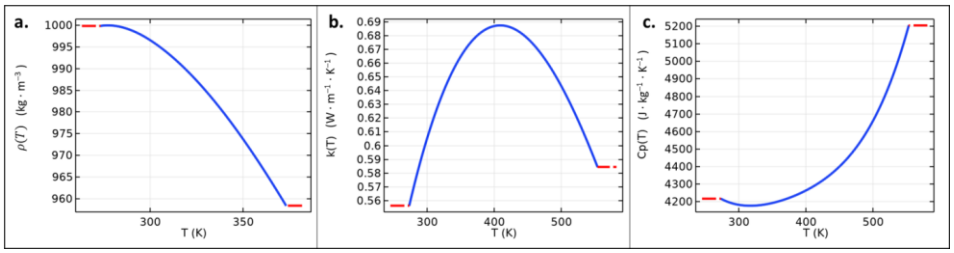

Figure 4. Temperature dependence of the water properties considered to be inside the cooling device: density (**a**), thermal conductivity (**b**) and heat capacity (**c**).

Verification

The computational domain was discretized using a mesh with tetrahedral elements, including a refined region where the laser light was applied, as shown in Figure 5a. See the Supplementary Material for mesh verification results and corresponding figures. The remaining computational domain was discretized with tetrahedral elements of "Normal" size, and the device wall and cooling water with "Fine" size elements (Fig. 5b). The final mesh comprised 134,132 individual elements. Quality measures were employed to assess the discretization of domains, ensuring reliability and precision in terms of symmetry, angles between nodes, volume-to-length balance, and uniformity in element sizes. These measures yielded average element quality of 0.66 for

skewness, 0.75 for the maximum angle, 0.79 for the volume-to-length ratio, and 0.7 for growth rate.

About time discretization, two time-dependent studies were set, the first from the beginning of the radiation until 20 s (total irradiation time), and the second one from 20 s to 250 s, without the laser heat source, to consider thermal latency. The time step was set to 1/20 of the irradiation time. For cases including PEC, an initial Stationary Study was conducted to attain a stable state for the cooling device and tissues around it.

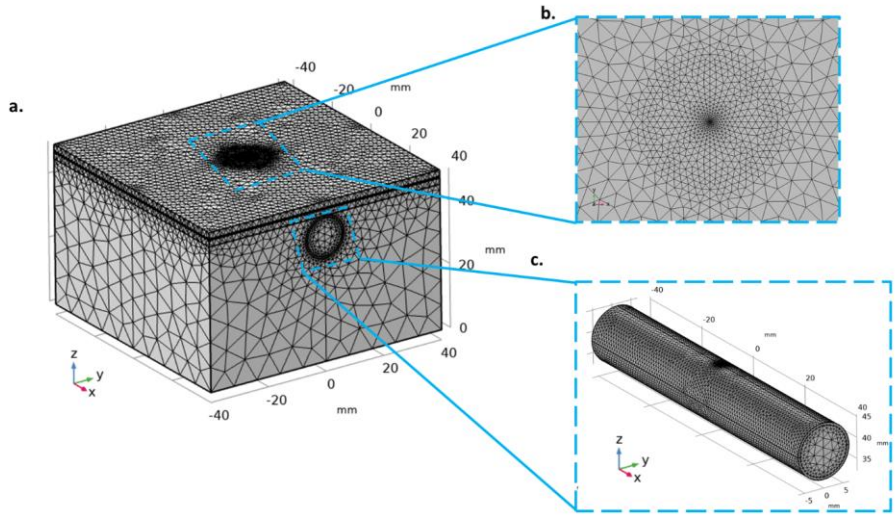

Figure 5. Model mesh and details of the relevant zones: Complete mesh (**a**) and refined mapped regions (**b** and **c**).

Validation

The model was adapted to the ex vivo conditions of the experiments by Nagase *et al* [10] (tissue temperature of 37 ºC, and absence of blood perfusion $Q_p = 0$). Due to the lack of knowledge about

the exact value of the radius of the laser applicator (r_i), we considered the range suggested by the manufacturer [5], and conducted a sensitivity study varying r_i from 6 to 10 mm. The lesion depth and surface width computed from FOD were compared to the values reported by Nagase *et al* [10], and we choose the value of r_i that best fits the experimental results in terms of lesion depth.

RESULTS

Figure 6 shows the comparison between the experimental results reported by Nagase *et al* [10] and the computer simulations for different values of the radius of the laser applicator (r_i). We found that r_i = 8 mm provided the smallest discrepancy (4%) with respect to the experimental value (3.95 mm vs. 4.1±0.4 mm). Overall, the computer model tended to underestimate the superficial width of the experimental lesion by around 25%. Since our study focuses on thermal damage caused in depth (esophagus), the lesion width at the surface level is a less relevant parameter.

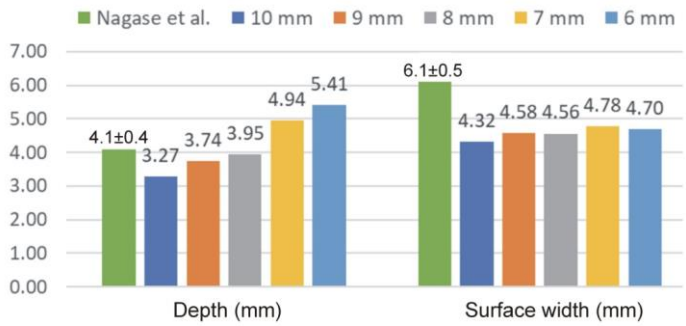

Figure 6. Comparison between experimental and computational results in terms of lesion (depth and surface width) at 8.5 W during 20 s. Experimental values correspond to the mean values reported by Nagase *et al* [10] using an ex vivo model. The computer simulations considered a range of values for the radius of the laser applicator (r_i) between 6 and 10 mm.

Once the radius of the laser applicator was fixed to r_i = 8 mm, maximum temperature and fraction of damage (FOD) was obtained for 20 different cases of tissue thicknesses, with and without PEC (Protection and Control, respectively). For all 20 cases without PEC, a thermal lesion equal to or greater than the thickness of the atrial wall was obtained. On the other hand, only six cases resulted in esophageal lesions, which are highlighted in Table 1 and overall corresponded with a short distance (≤ 3.5 mm) between esophagus and endocardial surface of the atrial wall, without PEC.. For the protection cases, no lesions for the esophagus were reached..

Figure 7 shows the distributions of fraction of damage at the end of the simulation (250 s) with black contours for 63% FOD, and temperature at the end of the laser pulse (20 s) for control and protection scenarios in the case 1 in which atrial wall is 1.0 mm and fat layer is 1.5 mm (see Table 1). It is observed that using PEC significantly alters the temperature distribution around the cooling device, producing at the end of the laser pulse temperatures that are clearly lower than in the control case (Fig. 7b). This translates into an absence of damage in the case of protection (see Fig. 7a). The absence of damage in the fat layer is due to the different parameters of the Arrhenius function defined for this tissue.

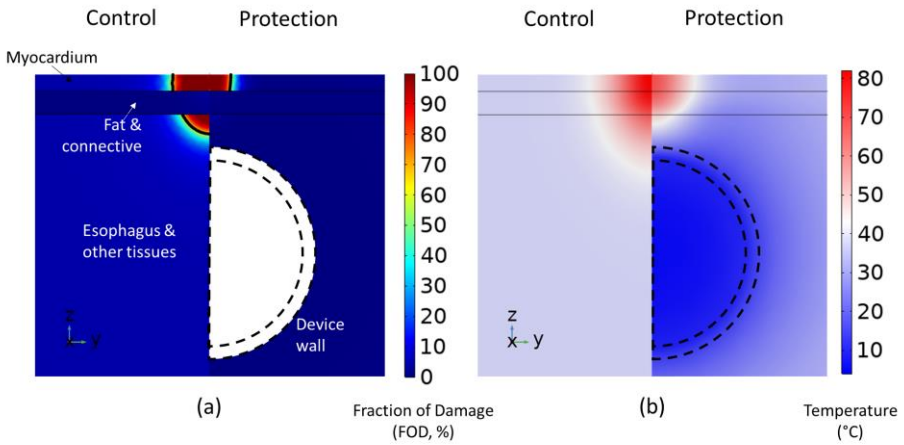

Figure 7. Distributions of fraction of damage FOD (**a**) at the end of the simulation (250 s) and temperature (**b**) at the end of the laser pulse (20 s) for control and protection scenarios (the plots correspond with the case 1 according to the data shown in Table 1).

Figure 8 shows the maximum temperature and fraction of damage (FOD) (%) in atrial wall and esophagus for the mentioned 6 cases without PEC in which esophagus damage occurred, in both protection and control scenarios. The thermal protection of the esophagus was evident in terms of reducing the maximum temperature reached in the esophagus in all cases, around 17 ºC less, as shown in Fig. 8c. This resulted in an important decrease in the FOD in the esophagus: values greater than60% in the control case (without protection) vs. values below 10% in the protection case (see Fig. 8d). Interestingly, the protective action of cooling hardly had any impact on the lesion created in the atrial wall in terms of fraction of damage (see Fig. 8a,b).

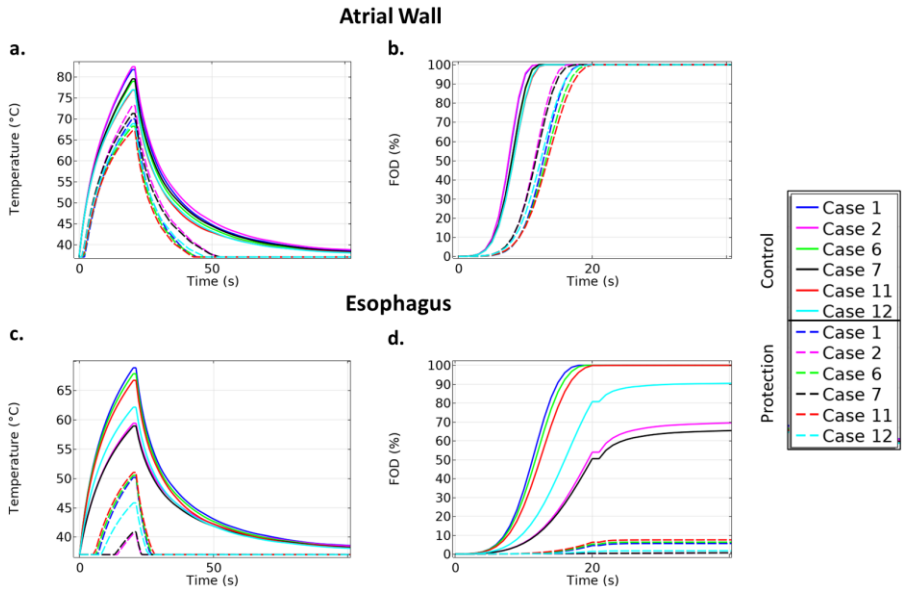

Figure 8. Progress of the maximum temperature and fraction of damage (FOD) during and after ablation in the atrial wall (**a,b**) and esophagus (**c,d**) for the three cases in which thermal damage occurred in the esophagus. Cases are shown for conditions both with and without proactive esophageal cooling (see Table 1 for details about the thickness of the involved tissues).

In control and protection cases, scenario 2 yielded the highest temperature in the atrial wall at 20 s, reaching a value of 82.45 ºC and 73.17 °C respectively;. For the esophagus, in control cases, scenario 1 yielded in the highest temperature with a value of 68.8 ºC, and in protection cases, scenario 11 reached the highest value of 50.99 ºC. For the atrial wall, the lower temperature was reached in case 11, and for the esophagus in case 2. There was no damage to the esophagus in any case in which the distance from the endocardium to the esophagus was greater than 3.5 mm.

Regarding the thermal dynamics, the maximum temperature in the tissue peaked at 20 s, just when the laser stops irradiating, suggesting that there is hardly any extra rise in temperature after ceasing to apply power (thermal latency). This can also be observed in the video file (Supplementary material) corresponding with the temperature distribution (control case), where the temperature starts to drop right at 20 s. However, due to the relatively slow decay of the maximum temperature (see Fig. 8a,c), the accumulated thermal damage computed with the Arrhenius function during the latency phase (after 20 s of laser application) increases, creating a lesion approximately of maximum 2.6 mm deeper (case 2).

DISCUSSION

In this modeling study we addressed for the first time the effect of laser ablation on the atrial wall for the purpose of treating AF, and the protective thermal effect of a cooling device located in the lumen of the esophagus. This is relevant from a clinical point of view since AEF is a critical event associated with the use of thermal ablative techniques in the vicinity of the esophagus, such as the posterior wall of the left atrium. Computational modeling aimed at exploring the factors of esophageal damage during radiofrequency (RF) ablation was initially proposed by Berjano and Hornero [6]. They concluded that thermal damage to the esophagus is probably caused by heat conduction from RF-heated cardiac tissue, and not by direct deposition of RF energy. In fact, the distance between the energy applicator and the esophagus appears to be the determining factor, which has motivated protective clinical techniques based on moving the esophagus as far away from the atrial wall as possible during ablation [25]. This protection technique can be considered "passive" compared to another "active" one based on forced cooling by circulating cold liquid inside the esophagus, also called PEC [26]. To this end, previous experimental [27,28] and

computer simulation [29] studies analyzed the operation of cooling systems based on an inflatable intraesophageal balloon. More recently, a new cooling device based on an esophageal flexible tube is being used clinically to protect the esophagus during RF ablation. In this case, computational modeling has already been used to explore the impact of this technology in terms of reducing thermal damage to the esophagus [7–9].

It is interesting to point out that the method of internally cooling a structure close to a hyperthermic ablation point in order to avoid collateral damage is widely used in different organs, such as the duodenum and veins in RF ablation of the pancreas [30] and bile duct during RF ablation of the liver [31]. Following the same methodology used in the aforementioned RF ablation studies, we planned a new study on the protective effect of this flexible tube-based device during cardiac ablation based on laser energy. This first-ever study of cardiac laser ablation and the effects of active esophageal cooling on esophageal injury found a significant reduction (to the point of elimination) of esophageal transmural injury when using PEC during laser ablation of the left atrium for the treatment of AF. Thermal protection of the esophagus resulted at least in part from reducing the maximum temperature reached in the esophagus. This allowed a significant decrease in the percentage of damaged esophagus, where values of maximum 60% were seen in the control case without the use of protection to values of 0% in the protected cases using PEC. This reduction in esophageal injury aligns well with what has been seen with the use of proactive esophageal cooling in RF ablation, both in pre-clinical and mathematical models [6–9] as well as in published clinical data [32,33]. Although the simplified geometric model has inherent limitations, recent clinical data have been presented with findings suggestive of a beneficial clinical effect from cooling during laser ablation, albeit without having histopathological correlation on tissue effects. Cooling significantly reduced mean procedure time, left atrial dwell time, and fluoroscopy time,

and increased percentage of time in rapid ablation mode, decreasing total therapy time, while reducing the recurrence rate of arrhythmia from 29% to 0% at 6-month follow-up [34].

It has become increasingly evident in the field of RF ablation that thermal latency is of greater importance to tissue effects than previously appreciated [35,36]. We found similar concerns in our study of laser ablation. Maximum temperature was found to have a relatively slow decay, such that the accumulated thermal damage (as computed by the Arrhenius equation) increases notably. The effect of this thermal latency is best seen in control cases (without protection from proactive esophageal cooling), and the effects are exacerbated in anatomical dimensions having a short distance between the endocardium and esophagus. The detrimental effects of this thermal latency were shown to be mitigated with the use of proactive esophageal cooling.

The action of PEC had minimal impact on the lesions created in the atrial wall, either in terms of the maximum temperature reached or the resulting fraction of damage. This effect is also seen in RF ablation, both in mathematical models [9] and in clinical data, where long-term follow-up has shown improvement in freedom from arrhythmia (post-ablation period in which the patient does not present with evidence of arrhythmia) with the use of PEC [37,38]. The presence of interspersed tissues between the atrial wall and the esophagus (such as the visceral and parietal layers of the fibrous pericardium, the pericardial space and serous fluid, and the pericardial fat), all of which have low or no tissue perfusion, likely contributes to this phenomenon by providing an effective insulating layer between the cooled esophagus and the myocardial tissue (atrial wall) being heated intentionally to induce targeted lesions.

Limitations

Although mathematical models can provide valuable insight into physical phenomena, they inevitably do not reflect all clinical findings. In the case of laser ablation, there are limited clinical or experimental data with which to compare our findings. Nevertheless, abundant data exist demonstrating the benefits of proactive esophageal cooling with RF ablation, and the findings here are in general agreement with these published data. Our model reproduces the interaction of the laser with the tissue and its resulting heating, and then, from the temperature reached and the exposure time, it estimates the thermal damage using the Arrhenius function.

Moreover, when the protection scenario using a PEC device was modeled, the velocity profile $\boldsymbol{u}$ of the cooled water flowing inside (see Eq. 2) was considered as constant, based on the device flow rate and area, and not as a parabolic velocity function that makes the velocity at the inner surface of the device wall tends to zero. This could modify the resulting heat transfer between the cooling device and the esophagus. Finally, our model does not account for other effects related to or resulting from esophageal thermal injury, such as changes to the downstream inflammatory cascade.

CONCLUSION

Proactive esophageal cooling (PEC) reduces the potential for esophageal injury without degrading the intended atrial lesions for a variety of tissue thicknesses. Thermal latency may influence lesion formation during laser ablation and may play a part in any collateral damage.

REFERENCES

1. Reynolds MR, Zheng Q, Doros G. Laser balloon ablation for AF: A systematic review and meta-analysis. J Cardiovasc Electrophysiol. 2018 Oct;29(10):1363-1370. doi: 10.1111/jce.13698.
2. Leung LWM, Akhtar Z, Sheppard MN, Louis-Auguste J, Hayat J, Gallagher MM. Preventing esophageal complications from atrial fibrillation ablation: A review. Heart Rhythm O2. 2021 Sep 22;2(6Part A):651-664. doi: 10.1016/j.hroo.2021.09.004.
3. Aupperle H, Doll N, Walther T, Kornherr P, Ullmann C, Schoon HA, Mohr FW. Ablation of atrial fibrillation and esophageal injury: effects of energy source and ablation technique. J Thorac Cardiovasc Surg. 2005 Dec;130(6):1549-54. doi: 10.1016/j.jtcvs.2005.06.052.
4. Weber HP, Schaur P, Sagerer-Gerhardt M. Use of Light Sensor and Focused Local Atrial Electrogram Recordings for the Monitoring of Thermal Injury to the Esophagus and Lungs During Laser Catheter Ablation of the Posterior Atrial Walls: Preclinical In Vitro Porcine and In Vivo Canine Experimental Studies. J Innov Card Rhythm Manag. 2019 Jul 15;10(7):3723-3731. doi: 10.19102/icrm.2019.100703.
5. HeartLight® X3 Endoscopic Ablation System Catheter, Endoscope, and Balloon Fill Media. Instructions for Use (06-4954 REV A). CardioFocus (Marlborough, MA, USA).
6. Berjano EJ, Hornero F. What affects esophageal injury during radiofrequency ablation of the left atrium? An engineering study based on finite-element analysis. Physiol Meas. 2005 Oct;26(5):837-48. doi: 10.1088/0967-3334/26/5/020.
7. Mercado M, Leung L, Gallagher M, Shah S, Kulstad E. Modeling esophageal protection from radiofrequency ablation via a cooling device: an analysis of the effects of ablation power and heart wall dimensions. Biomed Eng Online. 2020 Oct 12;19(1):77. doi: 10.1186/s12938-020-00821-z.
8. Montoya MM, Mickelsen S, Clark B, Arnold M, Hanks J, Sauter E, Kulstad E. Protecting the esophagus from thermal injury during radiofrequency ablation with an esophageal cooling device. J Atr Fibrillation. 2019 Feb 28;11(5):2110. doi: 10.4022/jafib.2110.
9. Mercado Montoya M, Gomez Bustamante T, Berjano E, Mickelsen SR, Daniels JD, Hernandez Arango P, Schieber J, Kulstad E. Proactive esophageal cooling protects against thermal insults during high-power short-duration radiofrequency cardiac ablation. Int J Hyperthermia. 2022;39(1):1202-1212. doi: 10.1080/02656736.2022.2121860.
10. Nagase T, Asano S, Yukino M, Mori H, Goto K, Ikeda Y, Iwanaga S, Muramatsu T, Mukaida H, Kato R, Matsumoto K. Influence of various energy settings and overlap ratios on size and continuity of lesions in a laser balloon ablation in vitro model. J Cardiovasc Electrophysiol. 2019 Aug;30(8):1330-1338. doi: 10.1111/jce.14040.
11. Sánchez-Quintana D, López-Mínguez JR, Macías Y, Cabrera JA, Saremi F. Left atrial anatomy relevant to catheter ablation. Cardiol Res Pract. 2014;2014:289720. doi: 10.1155/2014/289720.
12. Ho SY, Cabrera JA, Sánchez-Quintana D. Vagaries of the vagus nerve: relevance to ablationists. J Cardiovasc Electrophysiol. 2006 Mar;17(3):330-1. doi: 10.1111/j.1540-8167.2006.00364.x.
13. Pennes HH. Analysis of tissue and arterial blood temperatures in the resting human forearm. J Appl Physiol. 1948 Aug;1(2):93-122. doi: 10.1152/jappl.1948.1.2.93.
14. González-Suárez A, Pérez JJ, Irastorza RM, D'Avila A, Berjano E. Computer modeling of radiofrequency cardiac ablation: 30 years of bioengineering research. Comput Methods Programs Biomed. 2022 Feb;214:106546. doi: 10.1016/j.cmpb.2021.106546.
15. Hasgall PA, Di Gennaro F, Baumgartner C, Neufeld E, Lloyd B, Gosselin MC, Payne D, Klingenböck A, Kuster N, "IT'IS Database for thermal and electromagnetic parameters of biological tissues" Version 4.1, Feb 22, 2022, doi: 10.13099/VIP21000-04-1. itis.swiss/database.
16. Hsiao YS, Kumon RE, Deng CX. Characterization of Lesion Formation and Bubble Activities during High Intensity Focused Ultrasound Ablation using Temperature-Derived Parameters. Infrared Phys Technol. 2013 Sep 1;60:108-117. doi: 10.1016/j.infrared.2013.04.002.
17. Welch AJ. The thermal response of laser irradiated tissue. IEEE J Quantum Electronics. 1984 20 (12):1471-1481. doi: 10.1109/JQE.1984.1072339.

18. Saccomandi P, Schena E, Caponero MA, Di Matteo FM, Martino M, Pandolfi M, Silvestri S. Theoretical analysis and experimental evaluation of laser-induced interstitial thermotherapy in ex vivo porcine pancreas. IEEE Trans Biomed Eng. 2012 Oct;59(10):2958-64. doi: 10.1109/TBME.2012.2210895.
19. Splinter R, Svenson RH, Littmann L, Tuntelder JR, Chuang CH, Tatsis GP, Thompson M. Optical properties of normal, diseased, and laser photocoagulated myocardium at the Nd: YAG wavelength. Lasers Surg Med. 1991;11(2):117-24. doi: 10.1002/lsm.1900110205.
20. Siegman AE. Lasers. 1986. University Science Books (Melville, NY, USA). ISBN: 978-0-935702-11-8.
21. Yang D, Converse MC, Mahvi DM, Webster JG. Measurement and analysis of tissue temperature during microwave liver ablation. IEEE Trans Biomed Eng. 2007 Jan;54(1):150-5. doi: 10.1109/TBME.2006.884647.
22. Mohammadi A, Bianchi L, Korganbayev S, De Landro M, Saccomandi P. Thermomechanical Modeling of Laser Ablation Therapy of Tumors: Sensitivity Analysis and Optimization of Influential Variables. IEEE Trans Biomed Eng. 2022 Jan;69(1):302-313. doi: 10.1109/TBME.2021.3092889.
23. Yang D, Converse MC, Mahvi DM, Webster JG. Expanding the bioheat equation to include tissue internal water evaporation during heating. IEEE Trans Biomed Eng. 2007 Aug;54(8):1382-8. doi: 10.1109/TBME.2007.890740.
24. London RA, Eichler J, Liebetrudt J, Ziegenhagen L. Design of a protocol for combined laser hyperthermia – photodynamic therapy in the esophagus. Lasers in surgery: advanced characterization, therapeutics and systems X. Proc SPIE 2000; 3907:426. doi: 10.1117/12.386283.
25. Koruth JS, Reddy VY, Miller MA, Patel KK, Coffey JO, Fischer A, Gomes JA, Dukkipati S, D'Avila A, Mittnacht A. Mechanical esophageal displacement during catheter ablation for atrial fibrillation. J Cardiovasc Electrophysiol. 2012 Feb;23(2):147-54. doi: 10.1111/j.1540-8167.2011.02162.x.
26. Tsuchiya T, Ashikaga K, Nakagawa S, Hayashida K, Kugimiya H. Atrial fibrillation ablation with esophageal cooling with a cooled water-irrigated intraesophageal balloon: a pilot study. J Cardiovasc Electrophysiol. 2007 Feb;18(2):145-50. doi: 10.1111/j.1540-8167.2006.00693.x.
27. Lequerica JL, Berjano EJ, Herrero M, Melecio L, Hornero F. A cooled water-irrigated intraesophageal balloon to prevent thermal injury during cardiac ablation: experimental study based on an agar phantom. Phys Med Biol. 2008 Feb 21;53(4):N25-34. doi: 10.1088/0031-9155/53/4/N01.
28. Lequerica JL, Berjano EJ, Herrero M, Hornero F. Reliability assessment of a cooled intraesophageal balloon to prevent thermal injury during RF cardiac ablation: an agar phantom study. J Cardiovasc Electrophysiol. 2008 Nov;19(11):1188-93. doi: 10.1111/j.1540-8167.2008.01229.x.
29. Berjano EJ, Hornero F. A cooled intraesophageal balloon to prevent thermal injury during endocardial surgical radiofrequency ablation of the left atrium: a finite element study. Phys Med Biol. 2005 Oct 21;50(20):N269-79. doi: 10.1088/0031-9155/50/20/N03.
30. Fegrachi S, Molenaar IQ, Klaessens JH, Besselink MG, Offerhaus JA, van Hillegersberg R. Radiofrequency ablation of the pancreas with and without intraluminal duodenal cooling in a porcine model. J Surg Res. 2013 Oct;184(2):867-72. doi: 10.1016/j.jss.2013.04.068.
31. Feretis M, Wang Y, Zhang B, Liau SS. Biliary cooling during radiofrequency ablation of liver tumours close to central biliary tree: A systematic review and pooled analysis. Eur J Surg Oncol. 2021 Apr;47(4):743-747. doi: 10.1016/j.ejso.2020.09.033.
32. Leung LWM, Bajpai A, Zuberi Z, Li A, Norman M, Kaba RA, Akhtar Z, Evranos B, Gonna H, Harding I, Sohal M, Al-Subaie N, Louis-Auguste J, Hayat J, Gallagher MM. Randomized comparison of oesophageal protection with a temperature control device: results of the IMPACT study. Europace. 2021 Feb 5;23(2):205-215. doi: 10.1093/europace/euaa276.
33. Sanchez J, Woods C, Zagrodzky J, Nazari J, Singleton MJ, Schricker A, Ruppert A, Brumback B, Jenny B, Athill C, Joseph C, Shah D, Upadhyay G, Kulstad E, Cogan J, Leyton-Mange J, Cooper J, Tamirisa K, Omotoye S, Timilsina S, Perez-Verdia A, Kaplan A, Patel A, Ro A, Corsello A, Kolli A, Greet B, Willms D, Burkland D, Castillo D, Zahwe F, Nayak H, Daniels J, MacGregor J, Sackett M, Kutayli WM, Barakat M, Percell R, Akrivakis S, Hao SC, Liu T, Panico A, Ramireddy A,

Dewland T, Gerstenfeld EP, Lanes DB, Sze E, Francisco G, Silva J, McHugh J, Sung K, Feldman L, Serafini N, Kawasaki R, Hongo R, Kuk R, Hayward R, Park S, Vu A, Henry C, Bailey S, Mickelsen S, Taneja T, Fisher W, Metzl M. Atrioesophageal Fistula Rates Before and After Adoption of Active Esophageal Cooling During Atrial Fibrillation Ablation. JACC Clin Electrophysiol. 2023 Sep 12:S2405-500X(23)00673-4. doi: 10.1016/j.jacep.2023.08.022.

34. Doshi R, Kleinhans A. Esophageal cooling facilitates pulmonary venous antral isolation with laser balloon ablation. J Arrhythmia, 39: 13-268. https://doi.org/10.1002/joa3.12902.
35. Irastorza RM, d'Avila A, Berjano E. Thermal latency adds to lesion depth after application of high-power short-duration radiofrequency energy: Results of a computer-modeling study. J Cardiovasc Electrophysiol. 2018 Feb;29(2):322-327. doi: 10.1111/jce.13363.
36. Pérez JJ, González-Suárez A, Maher T, Nakagawa H, d'Avila A, Berjano E. Relationship between luminal esophageal temperature and volume of esophageal injury during RF ablation: In silico study comparing low power-moderate duration vs. high power-short duration. J Cardiovasc Electrophysiol. 2022 Feb;33(2):220-230. doi: 10.1111/jce.15311.
37. Leung LWM, Akhtar Z, Elbatran AI, Bajpai A, Li A, Norman M, Kaba R, Sohal M, Zuberi Z, Gallagher MM; on behalf of the IMPACT Study Group. Effect of esophageal cooling on ablation lesion formation in the left atrium: Insights from Ablation Index data in the IMPACT trial and clinical outcomes. J Cardiovasc Electrophysiol. 2022 Dec;33(12):2546-2557. doi: 10.1111/jce.15717.
38. Joseph C, Nazari J, Zagrodzky J, Brumback B, Sherman J, Zagrodzky W, Bailey S, Kulstad E, Metzl M. Improved 1-year outcomes after active cooling during left atrial radiofrequency ablation. J Interv Card Electrophysiol. 2023 Jan 21:10.1007/s10840-023-01474-3. doi: 10.1007/s10840-023-01474-3.